Sensors & Transducers, Vol. 227, Issue 11, November 2018, pp. 21-27

www.sensorsportal.com

Sensors & Transducers

Published by IFSA Publishing, S. L., 2018
http://www.sensorsportal.com

Atomistic Simulation of Structure and Dynamics in Crystallizing Germanium Thin Films

Yoshiaki KOGURE, Tomoko FUNAYAMA and Yasutaka UCHIDA
Teikyo University of Science, Adachi-ku, Tokyo, 120-0045, Japan
Tel.: +81-47-411-6265
E-mail: kogure@ntu.ac.jp

Received: 31 July 2018 /Accepted: 28 September 2018 /Published: 30 November 2018

Abstract: Low-temperature crystallization of germanium thin films has been simulated by means of molecular dynamics. Tersoff bond order potential was adopted for calculating the interactions between germanium atoms. Amorphous model was prepared by quenching the molten system at 1800 K. The model was consisted of about 1000, 5000 or 10000 atoms and free boundary condition was adopted. Then these amorphous systems were kept at temperatures, 400 K or 600 K, for 500,000 steps and crystallization was really observed. To investigate the atomistic process of crystallization the cross sectional view of the atomic configuration, the change of the mean potential energy, the radial distribution function and the trajectory of atomic displacement were evaluated. Boundary conditions between the sample and the substrate were investigated in detail.

Keywords: Germanium, Molecular dynamics, Crystallization, Amorphous, Radial distribution function, Tersoff potential.

1. Introduction

Metal induced crystallization has been extensively studied as a powerful method of crystallization. The present authors have been engaged in the study to fabricate the germanium thin films on the flexible substrates in the project to improve the yes/no device for the totally locked in state (TLS) patients, however it is not yet to be usable [1]. Problems are fitting and durability to use in daily life. In our experimental study germanium films are deposited at 60 □ and crystallized at 150 □ (423 K). However, the microscopic process of the mechanism of crystallization is not well understood in many cases. Molecular dynamics simulation using reliable interatomic potential is a powerful way to visualize microscopic processes of crystallization. A previous work has already been reported [2]. One of the present authors has been applied the molecular dynamics simulation on the studies of crystal defects and mechanical properties of metals [3]. The program code developed in the studies can be used in the present investigation.

2. Method of Simulation

The bond order potential function developed by Tersoff, *et al.*, is used in the simulation [4-5]. The potential energy depends on the bond length and bond angle. The potential energy is described as

$$E = \sum_i E_i, \qquad E_i = \frac{1}{2}\sum_{j \neq i} V_{i,j}, \tag{1}$$

$$V_{ij}(r) = f_{\mathrm{C}}(r)[\, f_{\mathrm{R}}(r) + b_{ij}\, f_{\mathrm{A}}(r)], \tag{2}$$

$$f_R = A\exp(-\lambda r)$$
$$f_A = -B\exp(-\mu r), \quad (3)$$

where b_{ij} is related to the coordination number and represent the many body nature of the potential. The truncation function $f_C(r)$ and other variables are described as

$$f_C(r) = \begin{cases} 1, & r < R \\ \frac{1}{2} + \frac{1}{2}\cos\left[\pi \frac{(r-R)}{S-R}\right], & R < r < S \\ 0, & r > S \end{cases}, \quad (4)$$

$$b_{ij} = \kappa_{ij}(1+\beta^n \zeta_{ij}^n)^{-1/2n},$$
$$\zeta_{ij} = \sum_{k \neq i,j} f_C(r_{ik}) g(\theta_{ijk}), \quad (5)$$
$$g(\theta_{ijk}) = 1 + \frac{c^2}{d^2} - \frac{c^2}{d^2 + (h - \cos\theta_{ijk})^2}$$

The force acting on an atom is calculated by differentiating the expression for energy, Eq. (1), by distance *r*. The equation of motion for an atom is solved by integrating the potential numerically by the Verlet algorithm. The time interval for the numerical integration is chosen to be $\Delta t = 1.0 \times 10^{-15}$ sec, which is much smaller than the period of the atomic thermal vibration.

The molecular dynamics simulations are performed by using a Fortran code developed the present authors and results are visualized by Visual Basic 6 (Microsoft).

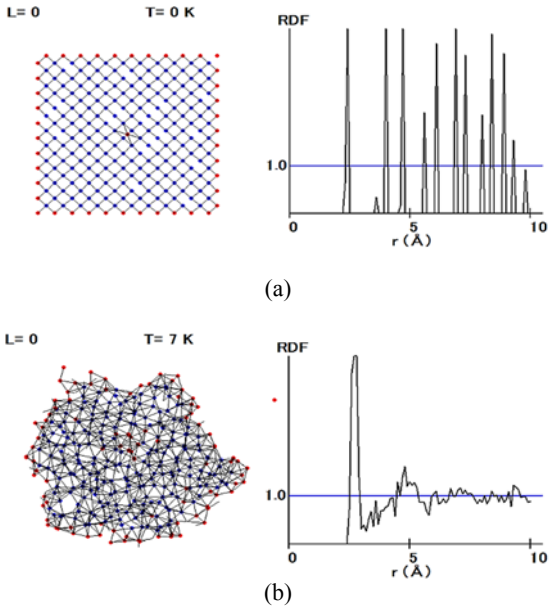

Fig. 1. Configuration of atoms (a) in perfect crystal and (b) in amorphous state. The radial distribution functions are shown in right hand side.

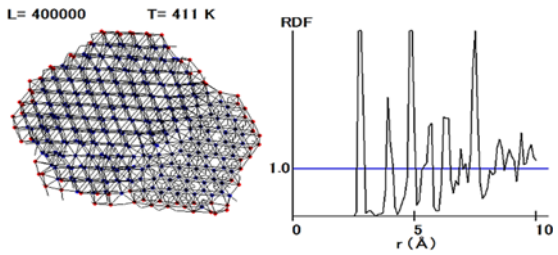

Fig. 2. Configuration of atoms and radial distribution function in crystallized state.

3. Results and Discussion

3.1. Particle-like Samples

For the simulation to investigate the fundamental mechanism of crystallization a small specimen consists of 1332 atoms is prepared. As an initial condition, atoms are arranged in diamond structure with {100} boundary surfaces as shown in Fig. 1 (a). The length of one side of cube is about 3 nm. The radial distribution function (RDF) of the structure is also shown in the right. The free boundary condition is adopted. Then the temperature is increased up to 1800 K. The molten state is quenched and amorphous state is realized.

The atomic structure and the RDF of amorphous state are shown in Fig. 1(b). A completely disordered structure of amorphous is seen.

The simulation of the low temperature crystallization starts from the amorphous state.

The temperature of the amorphous specimen was maintained at 411 K and 600 K. As an example of the structure of crystallized sample at 400 K is shown in Fig. 2.

It is seen that the sample is consisted of two grains and the RDF in right hand side shows a spike-like change characteristic of crystal is seen. The potential energy can be calculated by Eq. (1). The change of the potential energy is shown in Fig. 3. It monotonically decreases at the first 100 thousand steps, and the first crystallization is completed in this time domain. After that, the potential energy slightly increases and decreases again. Changes in grain structure occur in this region. The grain structures at typical time steps, (a) 100000, (b) 250000, (c) 400000, are also shown in the figure. The grain structure in the specimen is changing at the constant temperature. It is also seen that the outer shape of the sample also changes. It can be understood that the free surfaces of the specimen plays an important role in polycrystallization. In some cases, several tens of atoms were released from the sample to the outside, and crystallization occurred as a result of this. This may be related to collective motion of metal atoms promoting crystallization. Crystallization seems to have accidental features. Even in the simulation with the set temperature of 600 K, the same behavior was quantitatively observed.

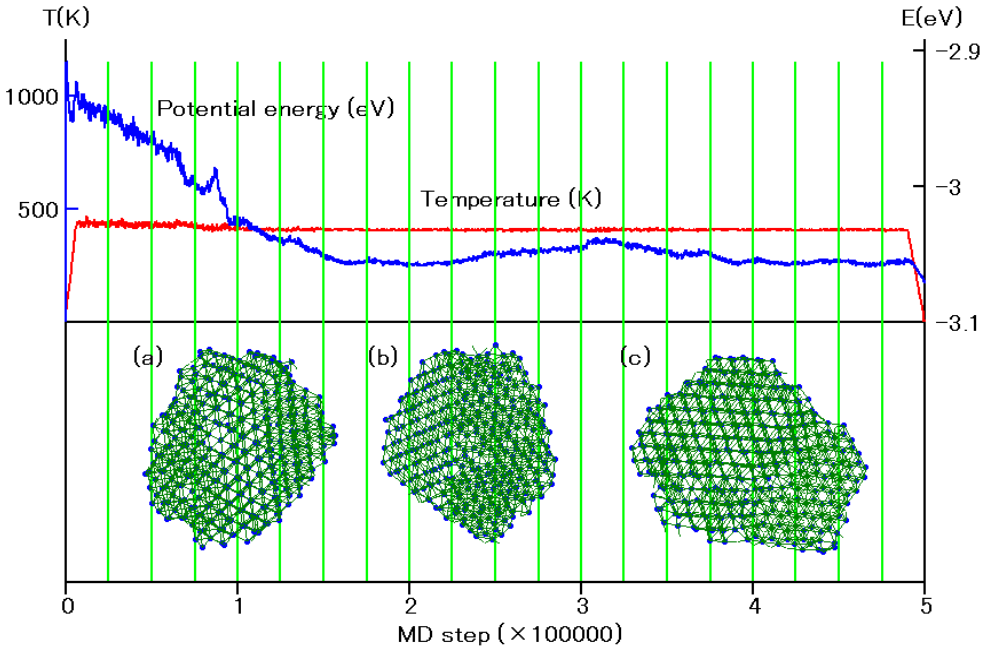

Fig. 3. Change of potential energy and typical grain structures at 400.

3.2. Plate-lile Sample A

A flat plate-like sample was prepared to simulate crystallization in the state close to a thin film. This is composed of 4852 atoms in the form of four particles arranged in the horizontal direction (Fig. 1 (a)) in the previous section. The temperature of this sample was raised to 1,800 K to bring it into a molten state, then quenched to realize an amorphous state (Fig. 4 (b)).

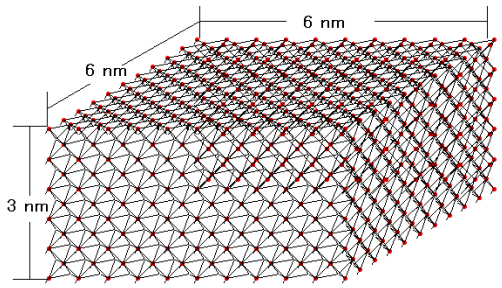

(a) Initial crystal

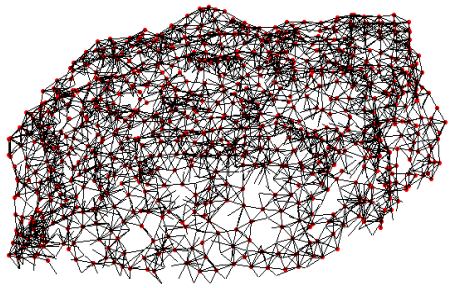

(b) Melted and quenched

Fig. 4. Preparation of plate-like sample A.

Simulation of polycrystallization was performed using this amorphous state as an initial state. Two types of boundary conditions are adopted between the substrate and the sample in the simulation:

1) The substrate and the sample are in close contact and atoms can slide on the surface,

2) Loose contact with the base plate (allowing withdrawal within 10 Å).

In the boundary condition (1), crystallization has hardly progressed because atoms are mostly fixed at the lower end of the sample. On the contrary, in the boundary condition (2), it can be seen that polycrystallization is more advanced because of the boundary condition close to the free surface even at the lower end. In order for crystallization to occur, a degree of freedom in the three-dimensional direction may be necessary between the sample and the substrate. Namely, the boundary condition is very important for the crystallization of thin films. The details of local crystallization in larger sample are described and discussed in the next section.

Fig. 7 shows the temporal change (step) of the average potential energy of atoms in the sample, with the blue lines for the boundary condition (i) and the red lines for the boundary condition (ii). The upper graph shows the results for 400 K and the lower graph shows the results for 600 K, and both have similar behavior. In the boundary condition (i), the potential energy is almost constant. The relaxation of atomic structure does not seem to occur. On the contrary, it can be seen that in the boundary condition (ii), the potential energy repeats an increase and decrease at initial several 10000 time steps. After the initial violent rise and fall, it is relaxed to a lower level. It seems that after 60000 time steps energy is reduced by polycrystallization.

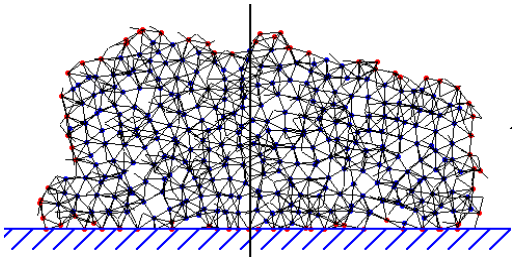

(a)

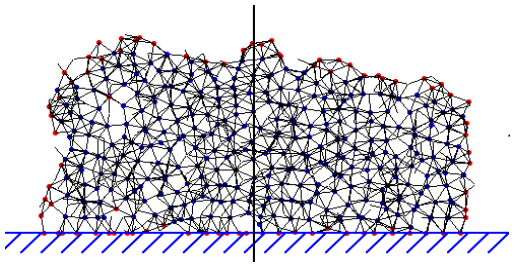

(b)

Fig. 5. Cross-sectional view of the plate-like sample. (a) initial smorphous state, (b) after annealing under boundary condition (1).

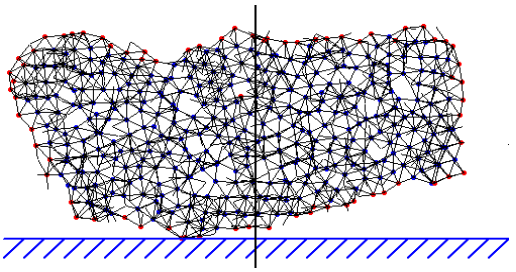

Fig. 6. Cross-sectional view of the plate-like sample after annealing under boundary condition (2).

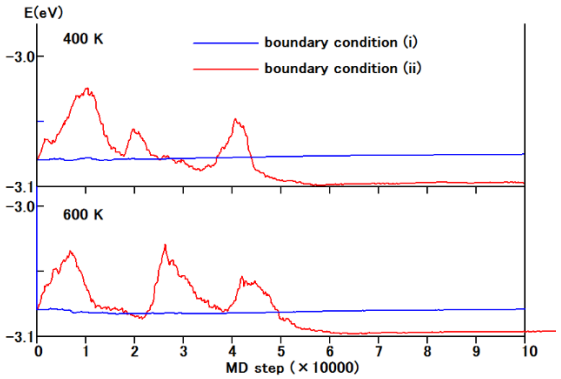

Fig. 7. Change of the mean potential energy.

The trajectories of the movement of atoms in the sample during the crystallization process under each boundary condition are shown in Fig. 8. Results for 400 K and 600 K are summarized. Small solid circles indicate the initial positions of each atom, and the curves following them indicate the trajectory of movement. In accordance with Fig. 7, the result of the boundary condition (i) is shown by blue lines and the result in the boundary condition (ii) is shown by red lines. In the boundary condition (i), it can be seen that small horizontal movements occur at both temperatures because only the motions parallel to the substrate are allowed. In the boundary condition (ii), large motions with rotation are seen at 400 K. At 600 K, large horizontal violent movements also occur.

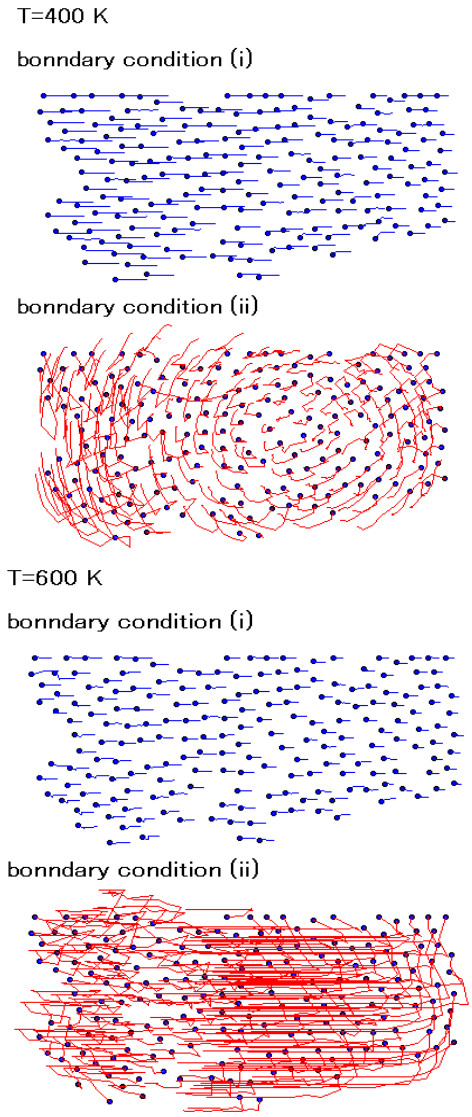

Fig. 8. Trajectory of atoms at 400 K and 600 K under the boundary conditions (i) and (ii).

Investigating the microscopic behaviors of atoms as described above is useful in studying the dynamical nature of atomistic mechanism of crystallization.

3.3. Plate-lile Sample B

A Larger sample was prepared to study the local motion state of the atoms in the crystallizing processes. The initial crystal has the same thickness as

the sample A in the previous section and has an area about twice as large, composed of 10572 atoms.

The dimensional drawing is as shown in Fig. 9(a). As before, the temperature was raised to 1800 K to molten state and then rapidly cooled down (quenched) to prepare a sample in an amorphous state at the starting sample B (Fig. 9(b)). In order to quantitatively investigate the process of partial crystallization of plate-like samples, 25 spherical domains are set in the sample as shown in Fig. 10.

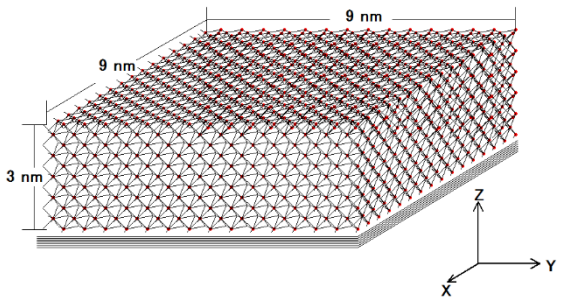

(a) Initial crystal

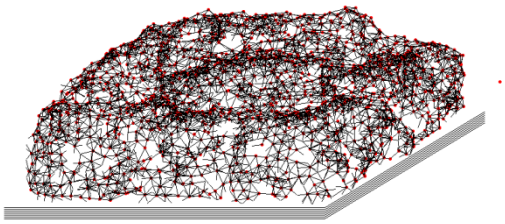

(b) Melted and quenched

Fig. 9. Preparation of plate-like sample B.

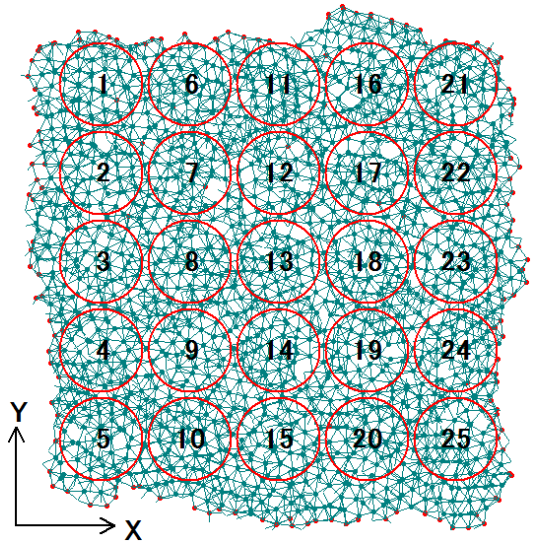

Fig. 10. Sample doains to track the atomic motion.

Each domain is spherical with a radius of 7 Å, which contains about 85 to 100 atoms. The arrangement and movement of the atoms contained in each region are tracked by molecular dynamics. Here, some of the results for 400 K annealing are described here.

As an example, Fig. 11 shows the changes of the atom array and the radial distribution function in domain 11. As the annealing progresses, the radial distribution function becomes sharp, and after 100000 steps, it shows nearly perfect crystal features. At the same time, it turns out that atomic arrangement is headed toward a regular array. In addition, in order to avoid complexity, atoms inside the region are not drawn, so there are parts where the space is seen bigger.

The trajectories of several selected atoms in the region are shown in Fig. 12. It is understood that the atoms are moving in random directions around the original positions.

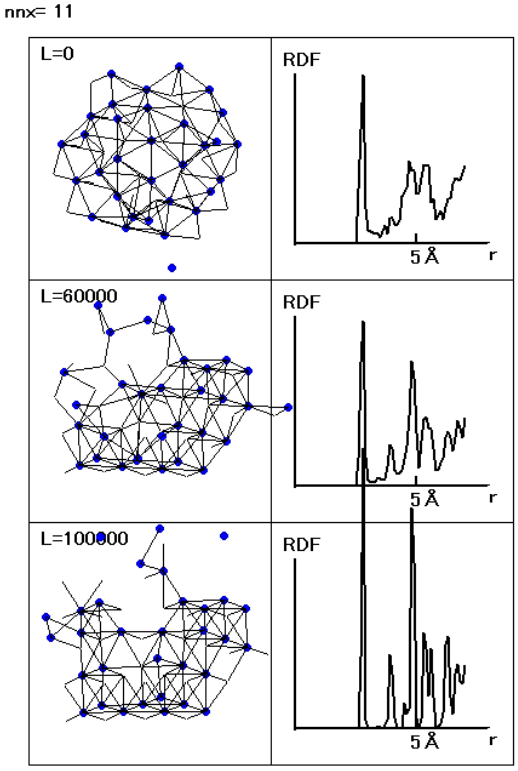

Fig. 11. AtomicConfiguration and RDF in domain 11.

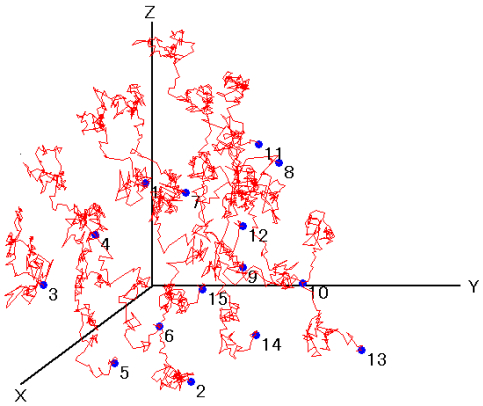

Fig. 12. Trajectory of atoms in domain 11.

Fig. 13 shows the temporal change of the displacement in the X direction. The numbers at the right end of each curve in the figure agree with the numbers attached to the atoms in the trajectory in Fig. 12. It is seen that the displacements of all atoms changes coherently with time through the annealing.

A similar analysis is performed for atoms in domain 19. Fig. 14 shows the changes of the atom array and the radial distribution function in domain 19. The radial distribution function does not change through 100000 steps and atomic arrangement does not show appreciable change. Namely, the crystallization does not happen in this domain.

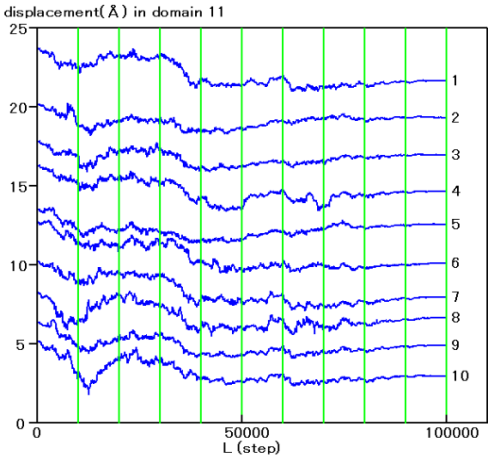

Fig. 13. Temporal change of displacement in X direction for atoms in domain 11.

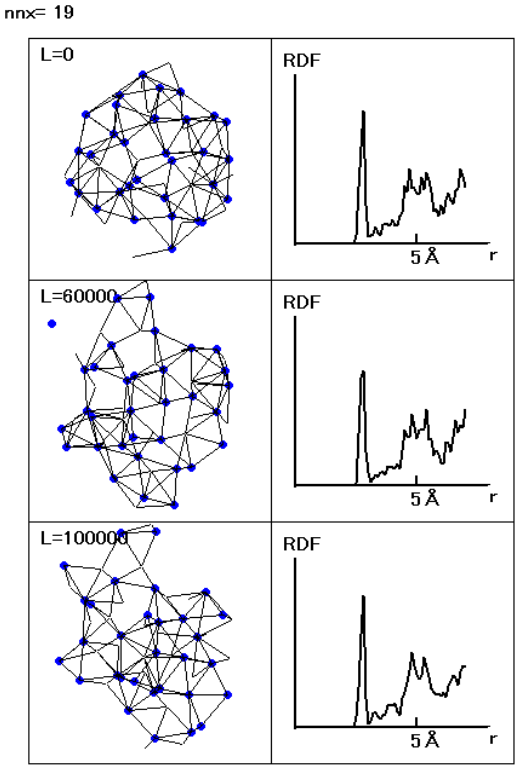

Fig. 14. AtomicConfiguration and RDF in domain 19.

The trajectory of atoms in domain 19 is shown in Fig. 15. Large displacements of atoms are seen of compared with Fig. 12. The temporal change of the displacement shown in Fig. 16 show rather irregular nature compared with the results for domain 11.

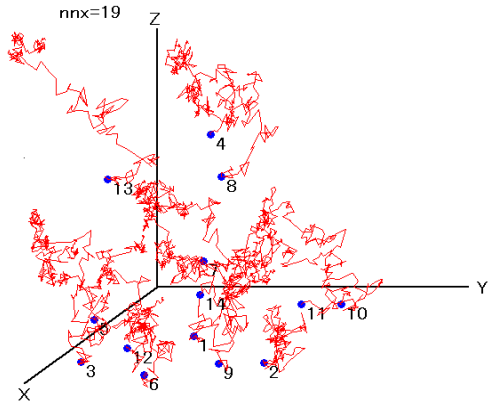

Fig. 15. Trajectory of atoms in domain 19.

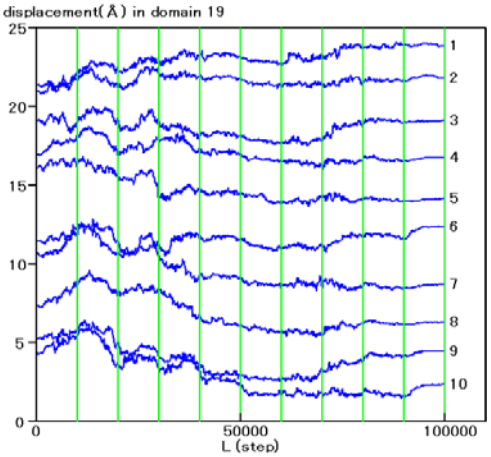

Fig. 16. Temporal change of displacement in X direction for atoms in domain 19.

Changes in the potential energy per atom in the domain 11 and 19 are compared in Fig. 17.

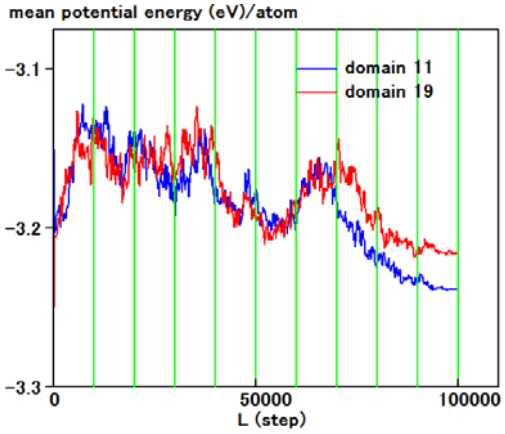

Fig. 17. Change of mean potential energy of Domain 11 and 19.

In both domains, the potential energy fluctuates drastically in the first half of annealing. After that, once it returns to the initial level, it rises again and then descends. The final energy is not so different from the initial value in the domain 19, but it is found to be low in the domain 11 where crystallization proceeds.

Similar inspections were performed in all 25 domains defined in Fig. 10, and it was found that crystallization proceeded in domain-1, -5, -6, -7, -11, -14, -15, -16, -21, and -24. Namely, crystallization was recognized in 40 % of domains. Here we set up a spherical domain with a radius of 7 angstrom as the first attempt, but it seems that the domains with a slightly flexible shape and size may be useful.

4. Conclusions

Low-temperature crystallization of amorphous Ge has been simulated by using the empirical Tersoff potential. The crystallization is observed at the temperatures 400 K and 600 K. The process of crystallization was monitored thorough the cross sectional view of the atomic structure and the RDF. Change in the potential energy associated with the crystallization was observed. Boundary conditions between the sample and the substrate were investigated in detail for the plate-like sample A, and a role of free space between the sample and the substrate was revealed. The non-uniform or heterogeneous nature of the crystallization was investigated in the larger plate-like sample B. The sample was divided to local domains and the structure and motion of atoms in the domains were compared. These results seem to be useful for the development of medical devices using germanium thin films.

References

[1]. Y. Uchida, T. Funayama, Y. Kogure and W. Yeh, Low-temperature Cu-induced poly-crystallization of electrodeposited germanium thin film on flexible substrate, *Physica Status Solodi*, 13, 2016, pp.864-867.

[2]. Y. Kogure, T. Funayama and Y. Uchida, Simulation of Low-Temperature Crystallization in Germanium Thin Films, in *Proceedings of the 1st International Conference on Microelectronic Devices and Technologies*, Barcelona, Spain, 20-22 June, 2018, pp. 65-68.

[3]. Y. Kogure and Y. Hiki, Atomistic Simulation of Shear Mode Deformation of Nanocrystalline Copper with Different Grain Sizes, *Materials Transactions*, 55-1, 2014, pp.64-68.

[4]. J. Tersoff, New empirical approach for the structure and energy of covalent systems, *Physical Review*, B 37 [12], 1988, pp. 6991-7000.

[5]. J. Tersoff, Modeling solid-state chemistry: interatomic potential for multicomponent systems, *Physical Review* B39, 1989, pp.5566-5568.